Progress In Electromagnetics Research, PIER 39, 47–59, 2003

FDTD MODELING OF A VIBRATING INTRINSIC REVERBERATION CHAMBER

N. K. Kouveliotis, P. T. Trakadas, and C. N. Capsalis

National Technical University of Athens
Department of Electrical and Computer Engineering
Division of Information Transmission Systems
and Material Technology
9, Iroon Polytechniou Str., 157 73, Zografou, Athens, Greece

Abstract—The field conditions inside a vibrating intrinsic reverberation chamber (VIRC) are examined. By the use of the Finite Difference Time Domain (FDTD) method, the field strength in the VIRC is calculated, and an investigation of the field uniformity and the field distribution is performed. The modes inside the cavity are excited by applying an appropriately modulated waveform on a dipoles gap. The use of this kind of waveform enables the study of the field conditions over a wide frequency range. On the contrary, an implementation of the field excitation with an unmodulated carrier would require a simulation of the FDTD method at each frequency of interest. Thus, a considerable reduction in the simulation time is achieved. The results presented, describing the field behavior inside the enclosure, agree with theory to a high degree.

1. INTRODUCTION

The use of reverberation chambers (either mode-tuned or mode-stirred chamber) for performing Electromagnetic Compatibility (EMC) measurements, has been of great interest over the last years. Their main features are the high field strength, the field uniformity and statistical isotropy and the fact that are easy to built and low cost structures. The International Electrotechnical Commission (IEC) has established a committee draft [1], which analytically describes the testing and measuring techniques that are evaluated during an emission or immunity test in a reverberation chamber.

The desirable field characteristics of a mode-stirred chamber are achieved by using a number of stirrers inside the shielded enclosure. The role of the stirrer is to efficiently "stir" the modes in the chamber by varying the boundary conditions and thus creating an overmoded cavity. This specified situation results in a completely random variation of the field values, which enables the chamber to behave with the previously discussed features. A stirrer usually appears in the form of a paddle wheel; however many different approaches have been proposed in the recent literature. Some examples are: the frequency stirring [2], the use of diffusers [3] or wires [4], the combined stirring using paddle wheels and corrugated walls [5], the moving wall mode-stirred chamber [6], the intrinsic reverberation chamber [7] and the vibrating intrinsic reverberation chamber (VIRC) [8, 9].

The VIRC will be studied in this paper. In this kind of chamber, instead of using the conventional paddle wheel, the modes are stirred by the random movement of the walls. The boundary conditions are significantly varied and consequently the basic reverberation chambers properties are obtained. The chamber used in our investigation, has two vibrating walls and the modes are excited using a dipole source. The Finite Difference Time Domain scheme [10, 11] is applied and the field strength is computed throughout the whole enclosure. A modulated waveform is applied on the dipoles gap, having a carrier with a specified center frequency and an appropriate envelope, which allows an observation over a wide frequency range after performing a Fourier transformation. This technique compensates for the major drawback of the FDTD algorithm, which is the computational burden, when simulating at certain frequencies, using an unmodulated carrier for excitation.

The FDTD method has been applied in the past for the case of mode-stirred chambers as described in [12–17]. In this study, after evaluating the FDTD scheme, the field uniformity is examined in the frequency domain according to the rules defined in the IEC

specification [1]. Moreover, the field distribution is compared to the theoretical results presented in the literature. In Section 2 the method used for modeling the VIRC is shown, where in Sections 3, 4 the results derived from the field uniformity and field distribution study are respectively presented.

2. VIRC MODELING METHOD

The VIRC with dimensions a (length), b (width), and c (height) is shown in Figure 1.

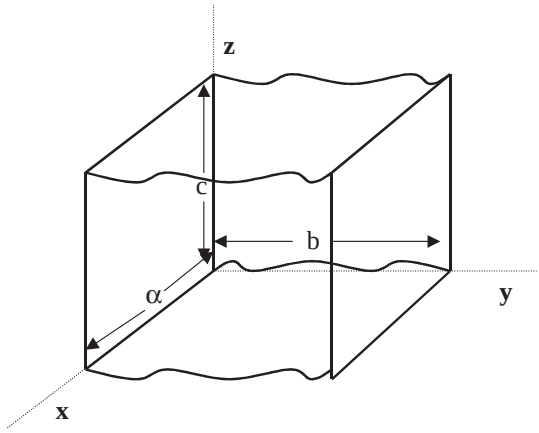

Figure 1. The vibrating intrinsic reverberation chamber.

It consists of a shielded enclosure with Perfect Electric Conducting (PEC) walls, two of which are vibrating, namely the $x = 0$, $x = a$ planes. The FDTD method will be applied to simulate the fields in this chamber. The special feature of the enclosure shown in Figure 1, is the presence of two vibrating rough surfaces. In order to implement them into the FDTD grid, we assume (without loss of generality) that they are one-dimensional and that they are represented by the structure depicted in Figure 2.

Each vibrating rough surface is thought to be of random height and is modeled as described in [18]. Concisely, the surface height as a function of an arbitrary point on the y axis, is considered to be of the form:

$$\chi(y_i) = \chi(y_{i-1}) + dy \cdot \tan(\varphi_{i-1}) \tag{1}$$

where $y_i = i \cdot dy$, $i = 1, \ldots, N$ represents N equidistant points on the y-axis separated by dy and φ_{i-1} is a random variable determining the

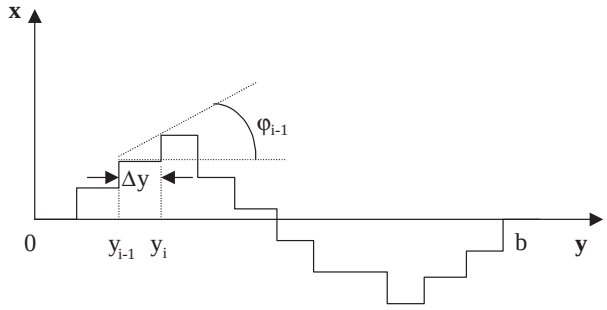

Figure 2. Rough surface modeling.

surface slope at the y_{i-1} segment. The slope of the surface at point y_i, is the tangent of an angle φ_i given by:

$$\varphi_i = \varphi_{i-1} + \omega_i \tag{2}$$

where ω_i is thought to be a random variable, uniformly distributed in a defined interval $[\varphi_{\min}, \varphi_{\max}]$. The procedure is initialized with the value $\chi(0) = 0$ and under the assumption that φ_0 is a random variable uniformly distributed in the range $[\varphi_{\min}, \varphi_{\max}]$. During the FDTD simulation, the tangential electric field components on the chambers walls are set equal to zero as the boundary conditions are applied.

The source used to excite the modes in the chamber is thought to be a thin wire dipole modeled as described in [19]. In that study, the near field physics of such a problem are included by assuming that the tangential electric field component on the dipole is zero except for the dipole's gap, where an appropriate excitation waveform is applied. Additionally, the field components near the dipole are calculated using the contour integral interpretations of Maxwell's equations [10]. Thus, for example the H_y component is expressed as follows [19]:

$$\begin{aligned} & H_y^{n+1/2}\left(i+\frac{1}{2}, j, k+\frac{1}{2}\right) \\ = \; & H_y^{n-1/2}\left(i+\frac{1}{2}, j, k+\frac{1}{2}\right) \\ & + \frac{dt}{\mu_0 dh}\left[E_x^n\left(i+\frac{1}{2}, j, k\right) - E_x^n\left(i+\frac{1}{2}, j, k+1\right)\right] \\ & + \frac{2dt}{\mu_0 dh \mathrm{In}\left(\frac{dh}{r_0}\right)}\left[E_z^n\left(i+1, j, k+\frac{1}{2}\right) - E_z^n\left(i, j, k+\frac{1}{2}\right)\right] \end{aligned} \tag{3}$$

where i, j, k are integers identifying the observation point, n is an

integer identifying the current observation time, dt, dh stand for the temporal and spatial increments respectively, μ_0 is the free space permeability, $r_0 = \frac{dh}{3}$ is the wire radius, and E_x, E_z are the x, z components of the electric field respectively. Considering a z-directed dipole, the $E_z^n\left(i, j, k+\frac{1}{2}\right)$ component on the dipole should be either equal to zero or to the excitation waveform $g(ndt)$ depending on k.

The excitation waveform applied on the dipoles gap, is considered to be of the form:

$$g(t) = \frac{\sin(2\pi W t)}{2\pi W t}\cos(2\pi f_c t) \tag{4}$$

where $2W$ is the chosen range width and f_c the center carrier frequency. After applying Fourier transformation [20] this waveform is represented in the frequency domain by the function:

$$G(f) = \frac{1}{4W}\left[rect\left(\frac{f-f_c}{2W}\right) + rect\left(\frac{f+f_c}{2W}\right)\right] \tag{5}$$

Assuming $f > 0$, we observe that in the frequency range $[f_c - W, f_c + W]$, the source provides a stable excitation of magnitude $\frac{1}{4W}$ and consequently, a simultaneous study of the chambers behavior at the frequencies consisting the specified range can be performed. As a result, compared to the case where an unmodulated carrier is used at a unique frequency, a significant reduction in the FDTD simulation time is achieved.

We have chosen to study a VIRC with initial dimensions of $a = 2m$, $b = 2m$ and $c = 2m$. For larger chamber's sizes, the FDTD simulation time becomes prohibitively huge, even when modern CPU's are used. According to the FDTD principles [10], two main conditions shall be considered whenever this method is evaluated. These are shown in equations (6), (7):

$$dt < \frac{dh}{c\sqrt{3}} \tag{6}$$

$$dh < \frac{\lambda_{\max}}{10} \tag{7}$$

where dt is the temporal segment, dh represents the size of the unit cubic cell, $\lambda_{\max}$ is the wavelength of the highest frequency desired and c is the speed of light in free space.

By applying the waveform described in equation (4), the highest frequency is $f_c + W$. We set $f_c = 1\,\text{GHz}$ and $W = 900\,\text{MHz}$, thus an appropriate choice of dt, dh is $dt = 2 \cdot 10^{-11}\text{sec}$ and $dh = 1.5\,\text{cm}$.

The dipole's length is $20dh$ and the width of the gap is dh while the center of the dipole is placed at the point with coordinates $(x, y, z) = (67dh, 20dh, 60dh)$. Also the surface characteristics are $dy = dh = 1.5cm$ and $[\varphi_{\min}, \varphi_{\max}] = [-20°, 20°]$ where $N + 1 = \frac{b}{dh} + 1 = 134$ points are considered on the y-axis.

The total simulation time is $50,000dt$ or 10^{-6} sec. Every $1000dt$ sec the profiles of the rough surfaces change resulting in 50 different cavity formulations and the pulse excitation is initialized. The field strength in the chamber is recorded between $500dt$ sec and $999dt$ sec for every cavity formulation to allow the field to become stable, after the alterations in the surfaces profiles. This procedure is called mode-tuned operation, to discriminate it from the "mode-stirred" operation [1, 21] where the stirrer moves continuously during the test.

Having calculated the field strength in the time domain, a Discrete Fourier Transformation (DFT) is applied, in order to examine the field strength in the frequency domain. The DFT is implemented separately for every cavity profile, resulting in 50 samples of the field strength for each frequency of interest. In the following sections, the field uniformity will be examined as well as the field distribution inside the chamber.

3. FIELD UNIFORMITY

The investigation of the field uniformity in our VIRC is performed according to the criteria defined in the IEC specification [1]. Eight points are considered forming a cubic volume of $(\lambda_{\min}/4)^3 m^3$, where $\lambda_{\min}$ is the wavelength of the lowest desirable frequency. The E_x, E_y, E_z values (representing the x, y, z components respectively of the electric field strength) at every point, were recorded during the FDTD simulation. For every cavity formulation (i.e., surfaces profiles), a DFT is applied resulting in a unique value of each of the calculated field components with respect to frequency. Therefore, 50 samples of each of the recorded electric field components at each frequency and at each point of the cubic volume are finally derived. The method used for calculating the chambers field uniformity is the standard deviation method [1]. Concisely, the maximum field strength at each of the eight sampling points for each of the three electric field components was calculated. These values are indicated by $E^i_{x\max}$, $E^i_{y\max}$, $E^i_{z\max}$, for the x, y, z electric field components respectively and $i = 1, \ldots, 8$ identifies the point number. Also a total data set E^i_{total} is formed for $i = 1, \ldots, 24$, by combining the three individual field components ($E^i_{x\max}$, $E^i_{y\max}$, $E^i_{z\max}$) from the eight locations. The standard

deviation is computed by:

$$\sigma = \alpha \sqrt{\frac{\sum (E_i - \langle E \rangle)^2}{n-1}} \tag{8}$$

where n is the number of samples, E_i stands for the $E^i_{x\,\max}$ or $E^i_{y\,\max}$ or $E^i_{z\,\max}$ or E^i_{total}, $\langle E \rangle$ is the average value over i of E_i, and $a = 1.06$ for $n \leq 20$ or $a = 1$ for $n > 20$. The standard deviation is expressed in dB relative to the mean by using the following expression:

$$\sigma(\text{dB}) = 20 \log \left(\frac{\sigma + \langle E \rangle}{\langle E \rangle} \right) \tag{9}$$

We applied the previously mentioned method to the results obtained by the FDTD simulation of the VIRC. We calculated four standard deviations, namely the $\sigma_x(\text{dB}), \sigma_y(\text{dB}), \sigma_z(\text{dB})$ and $\sigma_{total}(\text{dB})$ for $E^i_{x\,\max}$, $E^i_{y\,\max}$, $E^i_{z\,\max}$ and E^i_{total} respectively. The results for each frequency of interest are shown in Figure 3 where the field uniformity limitation proposed by the IEC specification is also depicted in the dotted line:

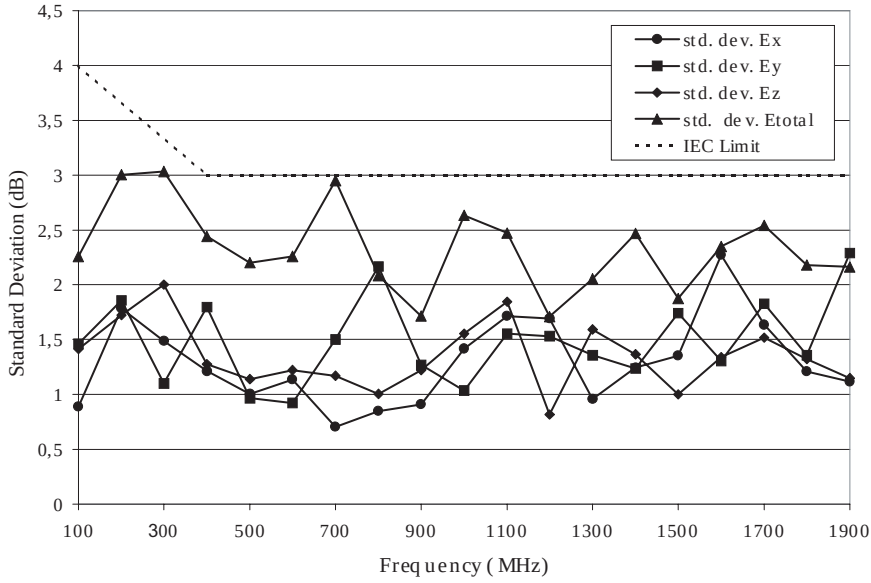

Figure 3. Standard deviation with respect to frequency.

As it is observed, the results obtained indicate that the performance of the chamber satisfies the uniformity criteria for every

frequency of investigation, and a slight improvement is achieved as frequency increases. Another interesting concern to be studied, is the variation of the standard deviation at a certain frequency, with the increase in the number of samples. The results for frequency of 1 GHz are shown in Figure 4:

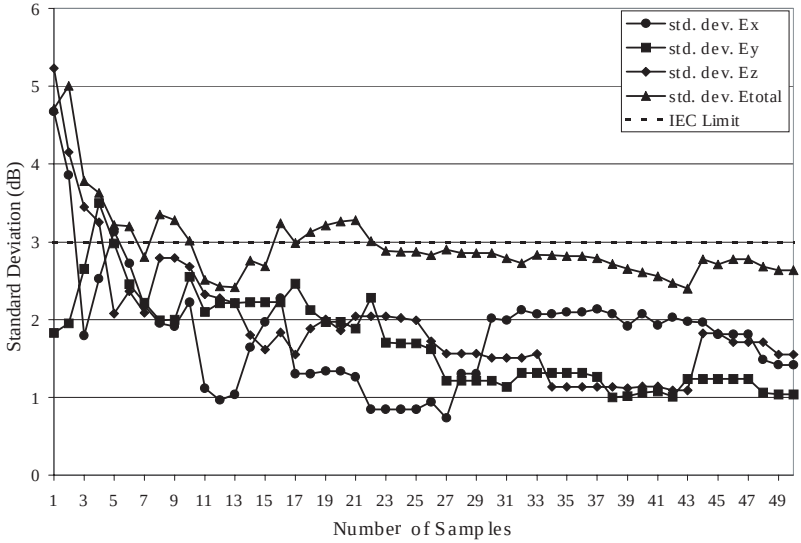

Figure 4. Standard deviation at 1 GHz with respect to the number of samples.

It can be noticed that a considerable decrease of the values of the standard deviation is obtained as the number of samples increases, and they seem to be stabilized after a number of samples. However, the desired field uniformity is achieved after a few samples (i.e., surfaces alterations), and that is interpreted by the fact that the chamber starts to behave like an intrinsic reverberation chamber even from the first surface alteration, which according to [7], can assure the proper chamber operation. Nevertheless, it is essential to introduce enough samples (about 30) for a better field uniformity.

4. FIELD DISTRIBUTION

As explicitly described in [22, 23], the electric field strength in a mode-stirred chamber is Rayleigh distributed when one polarization is considered, and chi distributed, when we assume polarization in the three axii. These field distributions refer to the case where there is

no direct path signal between the transmitter and receiver. In our case a direct path signal between the dipole antenna and the receiving point occurs and thus, the Rayleigh or chi distribution could no longer be applied. However this fast fading procedure can be adequately described by the Rice distribution. In order to perform this kind of study, we assume an arbitrary point in the chamber with dimensions $(x, y, z) = (42dh, 120dh, 42dh)$. We then examined the Probability Density Function (PDF) of the electric field strength at this certain point, with respect to frequency. In the following Table 1, a chi-square goodness-of-fit test between the simulated electric field distribution and the theoretical Rician distribution with $K = 1.2$, is presented at each frequency from 200 MHz to 1.9 GHz. The PDF at 100 MHz will be discussed later.

Table 1. X^2 goodness-of-fit Test with respect to frequency, level of significance $a = 0.05$, theoretical threshold=9.49.

Frequency (MHz)	X^2 Test
200	8.41
300	8.02
400	5.88
500	5.60
600	4.79
700	4.01
900	3.99
1100	3.21
1300	3.23
1500	3.02
1700	2.14
1900	1.93

The values show that the PDF of the electric field strength satisfies the theoretical Rice with $K = 1.2$, for all frequencies and this coincidence seems to improve, as frequency gets higher. A depiction of the coincidence at frequency of 900 MHz is shown in Figure 5 where the field strength values are normalized by their mean value.

At 100 MHz the electric field PDF of one polarization was found to satisfy the theoretical Rayleigh one, giving a value of the X^2 test of 4.96 where the theoretical threshold is 9.49 with significance level $a = 0.05$. In Figure 6, the comparison of the PDF of the normalized by

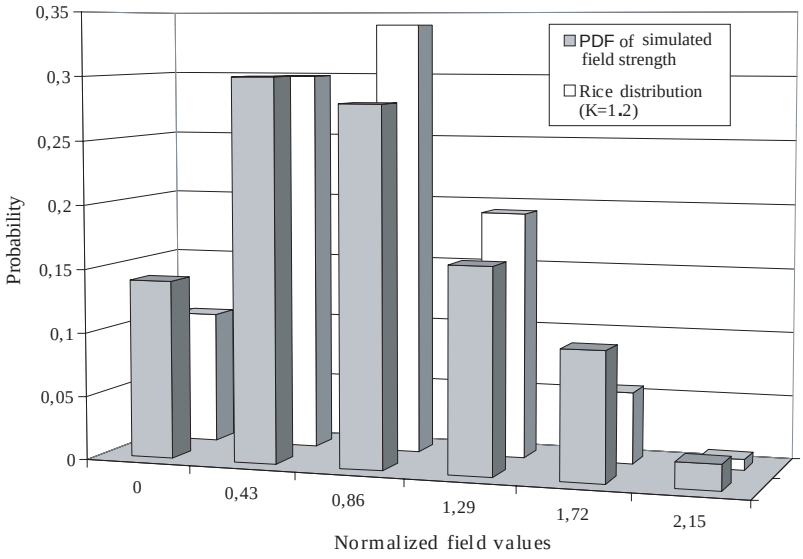

Figure 5. Probability density function at 900 MHz compared to Rice with $K = 1.2$.

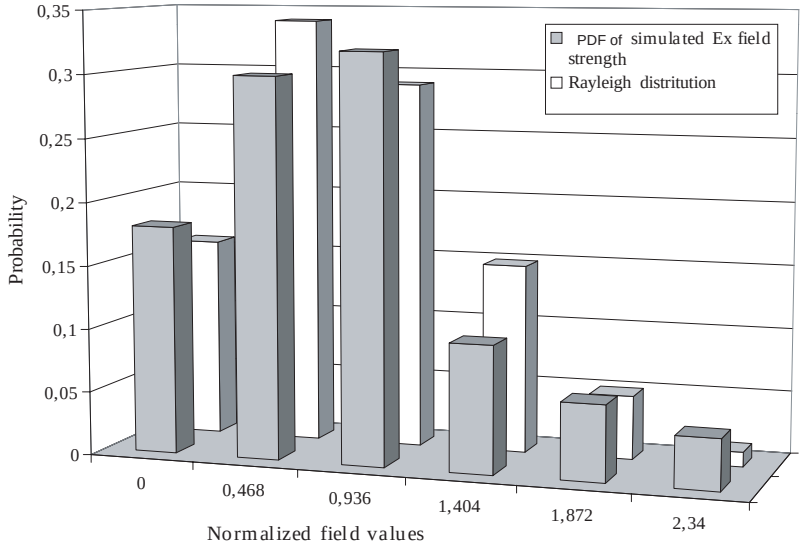

Figure 6. Probability density function at 100 MHz compared to Rayleigh.

the average value electric field strength of E_x polarization, is compared to the Rayleigh distribution.

The same results are also derived for the other polarizations. The previously mentioned observation arises from the fact that at 100 MHz the distance between the sampling point and the dipoles center is 1.56 m which is, less than the wavelength at this frequency. Consequently, the line-of-sight component of the transmitted signal does not appear to be so dominant compared to the reflected signals. Therefore the electric field strength could no longer be described by the Rice distribution and it is more adequate to describe it by the Rayleigh PDF.

5. CONCLUSIONS

The field uniformity together with the electric field distribution using the FDTD method was examined in a Vibrating Intrinsic Reverberation Chamber. By applying an appropriately modulated waveform on a dipoles gap, a considerable reduction in the simulation time is achieved, as a wide frequency range from 100 MHz to 1.9 GHz was simultaneously examined in a unique FDTD implementation. The field was found to be uniform over the whole frequency range and the uniformity was improved as the number of samples increased. In addition the PDF of the electric field strength was found to satisfy the Rician distribution as by using a dipole antenna there is a direct path signal between the transmitting and receiving point. The whole study marks out the usefulness of the VIRC as a modern application for performing EMC tests.

REFERENCES

1. Draft IEC 61000-4-21, 2001, *Electromagnetic Compatibility (EMC) Part 4: Testing and Measurement Techniques,* Section 21, Reverberation Chambers Test Methods.
2. Hill, D. A., "Electronic mode stirring for reverberation chambers," *IEEE Trans. Electromagn. Compat.,* Vol. 36, No. 4, 294–299, 1994.
3. Petirsch, M. and A. J. Schwab, "Investigation of the field uniformity of a mode-stirred chamber using diffusors based on acoustic theory, *IEEE Trans. Electromagn. Compat.,* Vol. 41, 446–451, 1999.
4. Perini, J. and L. S. Cohen, "An alternative way to stir the fields in a mode stirred chamber," *IEEE EMC Symposium,* 633–637, 2000.
5. Godfrey, E. A., "Effects of corrugated walls on the field uniformity

of reverberation chambers at low frequencies," *IEEE EMC Symposium,* 23–28, 1999.

6. Huang, Y. and D. J. Edwards, "An investigation of the electromagnetic field inside a moving wall mode-stirred chamber," *IEE Conference on EMC*, 115–119, Edinburgh, UK, 1992.
7. Lefering, F., "High field strength in a large volume: the intrinsic reverberation chamber," *IEEE EMC Symposium,* 24–27, 1998.
8. Leferink, F., J. C. Boudenot, and W. Etten, "Experimental results obtained in the vibrating intrinsic reverberation chamber," *IEEE EMC Symposium,* 639–644, 2000.
9. Leferink, F. and W. Etten, "Generating an EMC test field using a vibrating intrinsic reverberation chamber," *EMC Society Newsletter,* Spring 2001.
10. Taflove, A., *Computational Electrodynamics,* Artech House, Norwood, MA, 1995
11. Yee, K., "Numerical solution of initial boundary value problems involving maxwells equations in isotropic media," *IEEE Trans. Ant. Prop.,* Vol. 14, No. 3, 302–307, 1966.
12. Bai, L., L. Wang, B. Wang, and J. Song, "Reverberation chamber modeling using FDTD," *IEEE EMC Symposium,* 7–11, 1999.
13. Harima, K., "FDTD analysis of electromagnetic fields in a reverberation chamber," *IEICE Trans. Commun.,* Vol. E81-B, 1998.
14. Chung, S., J. Rhee, H. Rhee, and K. Lee, "Field uniformity characteristics of an asymmetric structure reverberation chamber by FDTD method," *IEEE EMC Symposium,* 2001.
15. Zhang, D., E. Li, and W. Yuang, "Study of independent sampling points in a reverberation chamber with two stirrers," *IEEE EMC Symposium,* 2001.
16. Rosengren, K., P. Kildal, C. Carlsson, and J. Carlsson, "Characterization of antennas for mobile and wireless terminals by using reverberation chambers: Improved accuracy by platform stirring," *IEEE AP-S Symposium,* 2001.
17. Hoijer, M., A. Andersson., O. Lunden, and M. Backstrom, "Numerical simulations as a tool for optimizing the geometrical design of reverberation chambers," *IEEE EMC Symposium,* 2000.
18. Kouveliotis, N. K., P. T. Trakadas, A. I. Stefanogiannis, and C. N. Capsalis, "Field prediction describing scattering by a one dimensional smooth random rough surface," *Electromagnetics,* Vol. 22, No. 1, 27–35, 2002.
19. Boonzaaier, J. J. and C. W. I. Pistorius, "Thin wire dipoles-

A finite-difference time-domain approach," *Electronics Letters,* Vol. 26, No. 22, 1891–1892, 1990.

20. Haykin, S., *Communications Systems,* Wiley, 1983.
21. Svetanoff, D., J. Weibler, R. Cooney, M. Squire, S. Zielinski, M. Hatfield, and M. Slocum, "Development of high performance tuners for mode-stirring and mode-tuning applications," *IEEE EMC Symposium,* 29–34, 1999.
22. Kostas, J. G. and B. Boverie, "Statistical model for a mode-stirred chamber," *IEEE Trans. Electromagn. Compat.,* Vol. 33, 366–370, 1991.
23. Hill, D. A., "Plane wave integral representation for fields in reverberation chambers," *IEEE Trans. Electromagn. Compat.,* Vol. 40, 209–217, 1998.